Computational Materials Science 155 (2018) 112–115

Contents lists available at ScienceDirect

Computational Materials Science

journal homepage: www.elsevier.com/locate/commatsci

Composition and processing dependent miscibility of P3HT and PCBM in organic solar cells by coarse-grained molecular simulations

Joydeep Munshi[a], Umar Farooq Ghumman[b], Akshay Iyer[b], Rabindra Dulal[c], Wei Chen[b], TeYu Chien[c], Ganesh Balasubramanian[a,*]

[a] Department of Mechanical Engineering & Mechanics, Lehigh University, Bethlehem, PA 18015, USA
[b] Department of Mechanical Engineering, Northwestern University, Evanston, IL 60208, USA
[c] Department of Physics & Astronomy, University of Wyoming, Laramie, WY 82071, USA

ARTICLE INFO

Keywords:
Coarse-grained molecular dynamics
Organic solar cells
Morphology
Bulkheterojunction

ABSTRACT

Organic solar cells (OSC) based on semiconducting polymers and electron-acceptor fullerene materials have shown tremendous promise in the past decade as an inexpensive and environment friendly renewable energy source. Morphology of the bulkheterojuction (BHJ) photoactive layer significantly affects the power conversion efficiency (PCE) of OSC devices. Mixtures of poly-(3-hexyl-thiophene) (P3HT) and phenyl-C61-butyric acid methyl ester (PCBM) have been a popular choice of organic materials due to their inexpensive synthesis and high thermal and mechanical stability. Composition and thermal processing significantly influence the miscibility of the donor-acceptor phases and the optimum device efficiency. We employ coarse-grained molecular dynamics simulations (CGMD) to investigate the miscibility of P3HT in PCBM with the Flory-Huggins interaction parameter, which suggests that exciton diffusion and transport are benefitted from an increase in both the PCBM mass loading and the P3HT chain length. Our predictions reveal that thermal annealing phase separates the polymers into an ordered phase that is beneficial for charge transport. Increased P3HT chain length and an equiweight mixture composition optimizes the miscibility and polymer domain sizes, suggesting processing conditions that can enhance power conversion.

Over the past decade, photovoltaic (PV) technologies have significantly advanced, demonstrating notable potential for solar energy conversion to electricity [1,2]. Amongst the different PV technologies explored, organic solar cells (OSCs) based on polymer-fullerene bulk heterojunction (BHJ) photoactive layers are attractive due to their low-temperature solution processability, light weight, environmental benignity, and flexibility. Though the power conversion efficiencies (PCE) of OSCs with BHJ architectures are relatively low as ~10% [3–5], a recent study with tandem structure composed of double BHJs further pushes the PCE up to 15% [6], a value often assumed market viable [7,8]. PCE depends on the morphology of BHJ and intermolecular interactions of the active layer constituents [9,10]. Poly-(3-hexyl-thiophene) (P3HT) and phenyl-C61-butyric acid methyl ester (PCBM) have emerged as the most promising constituent materials for the photoactive layer of organic solar cells due to the simple and inexpensive synthesis of P3HT and the notable thermal and mechanical stabilities of both P3HT and PCBM [11,12]. Experimental characterization of the three-dimensional (3D) morphology of the polymer-fullerene mixture is limited by the poor contrast rendered by electron microscopy, while, on the other hand, molecular simulations are able to reproduce detailed morphologies by deterministically sampling the atomic trajectories [13–17]. Here, we present results from coarse-grained molecular dynamics (CGMD) simulations of the thermal annealing of solvent-free mixture of P3HT and PCBM that compose the BHJ morphology. The Flory-Huggins model [18] is employed to calculate the miscibility of P3HT in PCBM for different compositions and degree of polymerization (i.e. P3HT chain lengths). We find that thermal annealing rearranges the P3HT chains into a relatively ordered and crystalline phase. Our results show that the miscibility, characterized by the χ parameter, decreases with increased PCBM mass loading and increased P3HT chain length, benefitting the exciton diffusion and transport. Our predictions are able to explain deterministically the earlier empirical experimental observations [19–23] on optimal P3HT:PCBM compositions to enhance PCE in OSCs.

P3HT, PCBM and Chlorobenzene (CB) molecules are modeled, shown in Fig. 1, using coarse-grained beads as described by the Martini force field [13,24] extended to polymers, fullerene and benzene rings [25–27]. While larger domains simulated for longer times can describe

* Corresponding author at: Packard Laboratory 561, 19 Memorial Drive West, Bethlehem, PA 18015, USA.
E-mail address: bganesh@lehigh.edu (G. Balasubramanian).

https://doi.org/10.1016/j.commatsci.2018.08.036
Received 2 July 2018; Received in revised form 13 August 2018; Accepted 17 August 2018

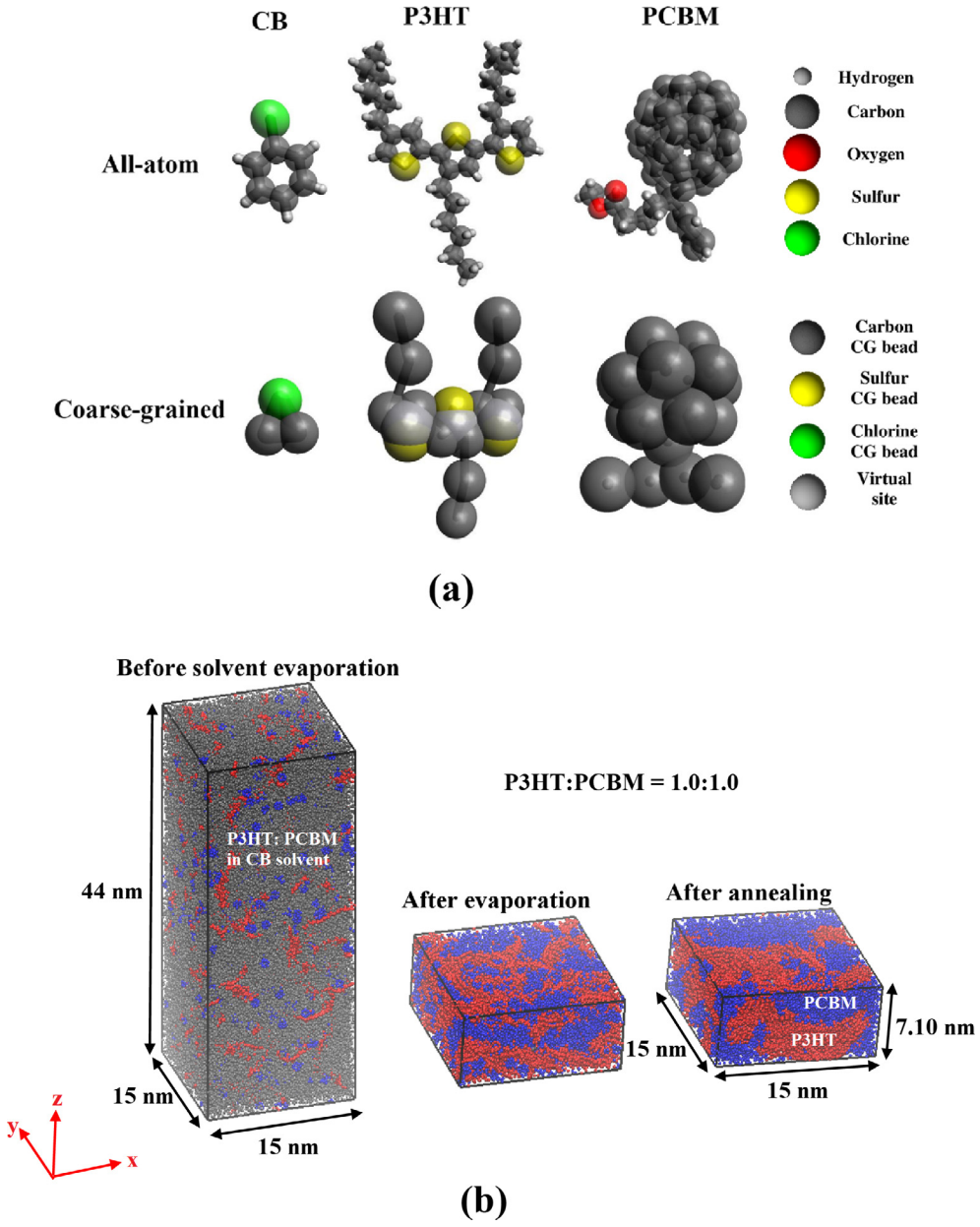

Fig. 1. (a) CB, P3HT (3-mer) and PCBM molecules and their respective coarse-grained forms are illustrated as described by the Martini CG model. 4 atoms are grouped together as a single CG bead except for the thiophene rings in P3HT and the fullerene cage in PCBM, where generally 3 atoms are modeled as a single CG bead. (b) A 3-dimensional representation of the simulation domain, before and after the solvent evaporation, and after complete thermal annealing. Note that thermal annealing does not change the dimension of the box.

the morphology of systems comparable to experimental samples, we believe our simulations are suitably able to offer the fundamental insights on the microstructure of these organic mixtures driven by intermolecular interactions. Solvent evaporation is simulated under an NPT (pressure constrained at 1 atm. and temperature at 298 K) ensemble by removing 1.25% of the CB molecules from the energy-minimized ternary mixture at regular time intervals of 3 ns (nanosecond), thus maintaining a constant vaporization rate. Thermal annealing of the solvent-free mixture is achieved by gradually increasing the temperature from 298 K to 698 K over three successive computational steps. Note that, experimentally the temperature during the annealing process typically reaches ~420 K [28]. The time scales for obtaining annealed morphologies in experiments (order of minutes [28]) is significantly different from that in the computations (order of microseconds [13]). CGMD simulations both in this work and in the literature [14,15,17,29–31], focus on the trends in morphology evolution under varying processing conditions. Hence, our use of a higher temperature is attributed towards realizing physically feasible morphologies and account for the differences in the degrees of freedom between simulations and experiments. The resulting morphology is characterized by discretizing the simulation box into cuboids (a.k.a. voxels) of dimensions consistent with the radius of the CG beads. Average domain size of the different phases are calculated from the total occupied volume of each of the pure P3HT (or PCBM) domains. The Flory-Huggins interaction parameter [18] (χ) is calculated from the local packing fraction of donor and acceptor phases by radical Voronoi tessellation scheme using the voro++ library [14,32].

P3HT: PCBM BHJ active layer can be considered as a solution of the electron-donor P3HT in the acceptor PCBM phase. A well-mixed solution of these two phases results in uniformly dispersed interpenetrating networks of P3HT and PCBM. According to the Flory-Huggins (FH) theory [18], the free energy of mixing the polymer-fullerene solution

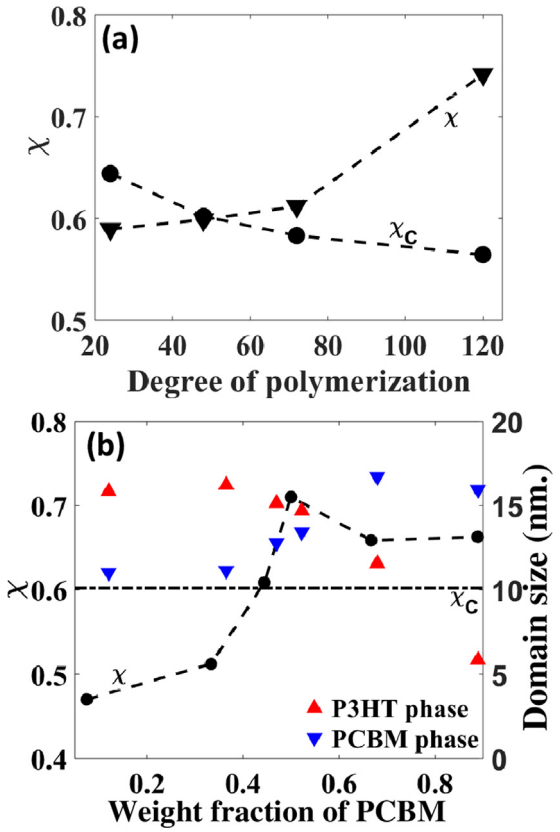

Fig. 2. (a) The variation of Flory-Huggins (FH) interaction parameter (χ) for different chain length sizes of P3HT in the polymeric solvent-free mixture. χ and χ_C (critical) both depend on the degree of polymerization. (b) The change in χ with weight fraction of PCBM for thermally annealed P3HT (48-mer): PCBM mixture shows that for weight ratio ~1:1, $\chi > \chi_C$ indicating immiscibility. Domain size of P3HT (red triangle) and PCBM (blue triangle) phases are almost equal at this composition indicating ideal exciton diffusion and charge generation. (For interpretation of the references to color in this figure legend, the reader is referred to the web version of this article.)

consists of the contributions from entropy and energy of mixing. The FH parameter χ is related to the energy of mixing at temperature T as, $\Delta U_{mix} = \chi\varphi_{PCBM}(1-\varphi_{PCBM})k_BT$, where ΔU_{mix} is the mixing energy, k_B is the Boltzmann constant and φ_{PCBM} is the PCBM volume fraction. When $\chi > \chi_C$, a critical threshold value, the solution starts to phase separate due to immiscibility of the two phases. $\chi_C \cong \frac{1}{2} + \frac{1}{\sqrt{N_{latt}}}$, where N_{latt} is a dimensionless volume occupied by P3HT with a chain length of N. χ_C is calculated as the product of N and the ratio of the volume occupied by a single P3HT monomer and a single CG bead volume [14].

Fig. 2(a) shows variation of χ with P3HT chain length for P3HT: PCBM weight ratio 1:0.8. The increase in χ with the degree of polymerization can be attributed to the higher tendency of longer chains to phase separate and hence lead to weaker miscibility in PCBM. However, on the other hand, χ_C being inversely proportional to chain length and volume occupied by P3HT chains, it decreases with increasing degree of polymerization. For the 1:0.8 P3HT: PCBM weight ratio, a crossover from $\chi < \chi_C$ to $\chi > \chi_C$ is noted for 48-mer P3HT. Hence, P3HT with chain length higher than 48-mers is suitable for OSCs due to enhanced charge transport through the pure P3HT and PCBM domains in the BHJ. In addition, using the 48-mer P3HT, a variation in the composition affects χ.

The trend of increasing χ with PCBM mass loading has been recorded in previous experiments [19,22,23] as well as in computations [29]. Domain size can be directly related to mixing of two phases as higher immiscibility (higher value of χ) leads to a higher domain size. The domain size predictions from our simulations are in agreement with experimental [20,21] and earlier computational (LPC force field) results [17]. We find the domain sizes of P3HT and PCBM to be almost equal (when interaction parameter, $\chi > \chi_C$, indicating immiscibility) for a 1:1 weight ratio (i.e. PCBM weight fraction of 0.5 in Fig. 2(b)) indicating optimum exciton diffusion and charge mobility. Hence, it is desirable to have BHJ active layers with P3HT: PCBM weight ratio higher than 1:0.8 in order to have better charge percolation and charge mobility in the respective phases. With increasing PCBM mass loading in the mixture, χ increases until it reaches a maximum at 50% weight fraction. However, increasing PCBM mass fraction beyond 0.5 results in diminished P3HT domain sizes, which may result in isolated P3HT domains that do not percolate into networks for hole collection at electrode.

Fig. 3 illustrates the variation in χ with the duration of thermal annealing for 1:1 weight ratio of P3HT (48-mer): PCBM. $\chi < \chi_C$ indicates miscibility at the beginning of the simulations; we find P3HT

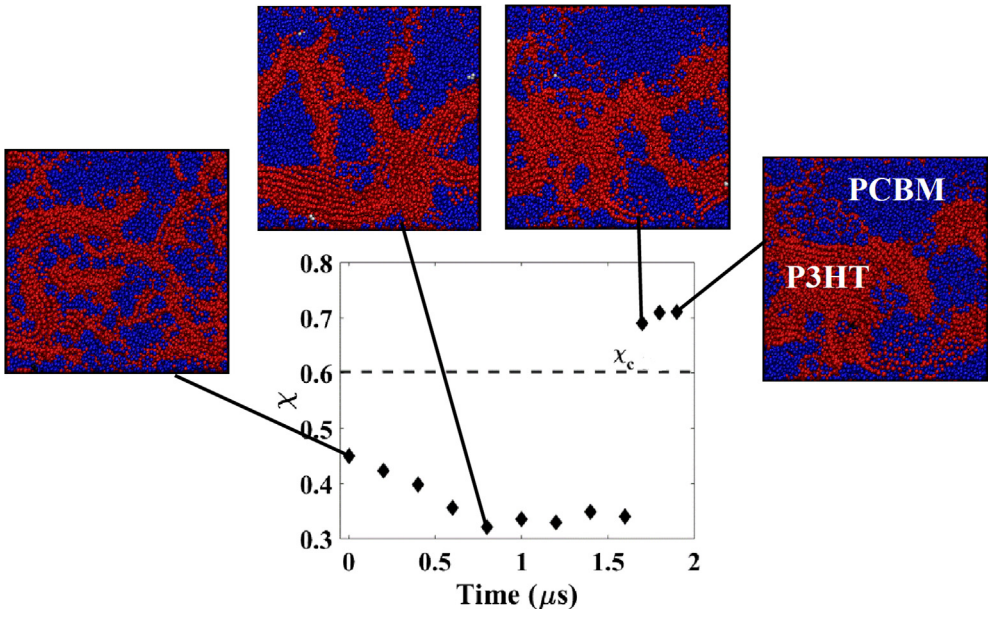

Fig. 3. The variation in χ is presented as a function of the duration of thermal annealing simulation for 1:1 weight ratio of P3HT (48-mer): PCBM. Temperature of the mixture is increased gradually from 298 K to 698 K. Initially, solvent free mixture at 298 K is observed to have a $\chi < \chi_C$ indicating miscibility of P3HT in PCBM. With increase in temperature, P3HT: PCBM mixture behaves more like a melt and χ further decreases and attains a minimum at 698 K (at time ~0.75 μs). χ increases upon quenching of the mixture (T = 298 K). Note that χ before and after annealing is significantly different, indicating a crossover from $\chi < \chi_C$ (miscibility) to $\chi > \chi_C$ (immiscibility). The morphologies for the P3HT (red): PCBM (blue) mixture before, during and after the annealing process also concur with the predicted behaviors. (For interpretation of the references to color in this figure legend, the reader is referred to the web version of this article.)

domain to be dispersed in PCBM from the morphology of the solvent free P3HT: PCBM mixture. Over time, P3HT: PCBM mixture is exposed to high temperature (up to 698 K). After ~0.75 μs, χ attains its lowest value. Decrease in χ during annealing can be attributed to the fusing of the P3HT: PCBM mixture due to the high temperatures. We allow the temperature of the simulation cell to decrease after 1.6 μs, whence χ increases upon quenching of the mixture (T = 298 K). At this stage, P3HT chains rearrange themselves in PCBM to form highly ordered and crystalline pure P3HT domains at around 1.7 μs. However, due to the annealing, the final morphology results in $\chi > \chi_C$, denoting immiscibility. Note that the value of χ before and after annealing is significantly different. Annealing enhances the crystallinity of P3HT domains and PCBM molecules are forced to phase separate, as evident from the morphology for the P3HT: PCBM mixture after annealing.

In summary, P3HT:PCBM bulk heterojunction morphology is simulated from a mixture of P3HT and PCBM solvated in Chlorobenzene using CGMD simulations. Calculation of the Flory-Huggins interaction parameter (χ) reveals that annealing of P3HT: PCBM mixture significantly increases the performance of the device due to increased crystallinity and decreased miscibility of the two phases. Processing dependent parameters such as weight ratio of P3HT and PCBM and the degree of polymerization of semiconducting P3HT influence χ. Critical interaction parameter χ_C is inversely proportional to polymer chain length. A crossover of $\chi < \chi_C$ to $\chi > \chi_C$ at a polymer chain length of 48 suggests use of P3HT with chain length greater than 48-mers will enhance performance. χ also varies with composition of P3HT and PCBM. With increasing mass loading of PCBM, χ increases and the mixture switches from miscibility to immiscibility at ~1:0.8 weight ratio where χ is almost equal to its critical value for the particular P3HT chain length. From calculations of χ and domain size, we conclude that weight ratios ~1:1 should be ideal for optimum exciton diffusion and charge percolation. Once integrated with structure-performance simulations as shown in our earlier efforts [33,34], the method presented here will allow virtual material design in which both the microstructure and the corresponding processing conditions can be optimized.

Data availability

The raw/processed data required to reproduce these findings cannot be shared at this time as the data also forms part of an ongoing study.

CRediT authorship contribution statement

JM performed the CGMD simulations and associated analyses. JM and GB wrote the manuscript. UFG, AI, RD, WC and TC edited the manuscript, and helped with analyses of the results and responses to the reviews. WC, TC and GB conceived the project.

Acknowledgments

This material is based on the work supported by the National Science Foundation (NSF) under Award Nos. CMMI-1662435, 1662509 and 1753770. Any opinions, findings, conclusions or recommendations expressed in this material are those of the authors' and do not necessarily reflect the views of the NSF.

References

[1] Sarah Kurtz, Nancy Haegel, Ronald Sinton, Robert Margolis, Nat. Photonics 11 (2017) 3.
[2] Chun Sing Lai, Youwei Jia, Loi Lei Lai, Zhao Xu, Malcolm D. McCulloch, Kit Po Wong, Renew. Sustain. Energy Rev. 78 (2017) 439.
[3] Martin Kaltenbrunner, Matthew S. White, Eric D. Glowacki, Tsuyoshi Sekitani, Takao Someya, Niyazi Serdar Sariciftci, Siegfried Bauer, Nat. Commun. 3 (2012) 770.
[4] Michael R. Lee, Robert D. Eckert, Karen Forberich, Gilles Dennler, Christoph J. Brabec, Russell A. Gaudiana, Science 324 (5924) (2009) 232.
[5] Gang Li, Rui Zhu, Yang Yang, Nat. Photonics 6 (2012) 153.
[6] Xiaozhou Che, Yongxi Li, Yue Qu, Stephen R. Forrest, Nat. Energy 3 (5) (2018) 422.
[7] Joseph Kalowekamo, Erin Baker, Sol. Energy 83 (8) (2009) 1224.
[8] Jianqi Zhang, Lingyun Zhu, Zhixiang Wei, Small Methods 1 (12) (2017) 1700258.
[9] Ye Huang, Edward J. Kramer, Alan J. Heeger, Guillermo C. Bazan, Chem. Rev. 114 (14) (2014) 7006.
[10] Nicholas E. Jackson, Brett M. Savoie, Tobin J. Marks, Lin X. Chen, Mark A. Ratner, J. Phys. Chem. Lett. 6 (1) (2015) 77.
[11] Andrew T. Kleinschmidt, Samuel E. Root, Darren J. Lipomi, J. Mater. Chem. A 5 (23) (2017) 11396.
[12] Brian R. Saunders, Michael L. Turner, Adv. Colloid Interface Sci. 138 (1) (2008) 1.
[13] Riccardo Alessandri, Jaakko J. Uusitalo, Alex H. de Vries, Remco W.A. Havenith, Siewert J. Marrink, J. Am. Chem. Soc. 139 (10) (2017) 3697.
[14] Jan-Michael Y. Carrillo, Rajeev Kumar, Monojoy Goswami, Bobby G. Sumpter, W. Michael Brown, Phys. Chem. Chem. Phys. 15 (41) (2013) 17873.
[15] David M. Huang, Roland Faller, Khanh Do, Adam J. Moulé, J. Chem. Theory Comput. 6 (2) (2010) 526.
[16] Eric Jankowski, Hilary S. Marsh, Arthi Jayaraman, Macromolecules 46 (14) (2013) 5775.
[17] Cheng-Kuang Lee, Chun-Wei Pao, Chih-Wei Chu, Energy Environ. Sci. 4 (10) (2011) 4124.
[18] M. Rubinstein, R. Colby, Polymer Physics, Oxford University Press, 2003.
[19] Huipeng Chen, Raghavendra Hegde, J. Browning, M.D. Dadmun, Phys. Chem. Chem. Phys. 14 (16) (2012) 5635.
[20] Brian A. Collins, Eliot Gann, Lewis Guignard, Xiaoxi He, Christopher R. McNeill, Harald Ade, J. Phys. Chem. Lett. 1 (21) (2010) 3160.
[21] Lawrence F. Drummy, Robert J. Davis, Diana L. Moore, Michael Durstock, Richard A. Vaia, Julia W.P. Hsu, Chem. Mater. 23 (3) (2011) 907.
[22] Derek R. Kozub, Kiarash Vakhshouri, Lisa M. Orme, Cheng Wang, Alexander Hexemer, Enrique D. Gomez, Macromolecules 44 (14) (2011) 5722.
[23] Ji Sun Moon, Jae Kwan Lee, Shinuk Cho, Jiyun Byun, Alan J. Heeger, Nano Lett. 9 (1) (2009) 230.
[24] Siewert J. Marrink, D. Peter Tieleman, Chem. Soc. Rev. 42 (16) (2013) 6801.
[25] Luca Monticelli, J. Chem. Theory Comput. 8 (4) (2012) 1370.
[26] Emanuele Panizon, Davide Bochicchio, Luca Monticelli, Giulia Rossi, J. Phys. Chem. B 119 (25) (2015) 8209.
[27] Martin Vögele, Christian Holm, Jens Smiatek, J. Chem. Phys. 143 (24) (2015) 243151.
[28] Trung Dang Minh, Lionel Hirsch, Guillaume Wantz, Adv. Mater. 23 (31) (2011) 3597.
[29] Jan-Michael Y. Carrillo, Zach Seibers, Rajeev Kumar, Michael A. Matheson, John F. Ankner, Monojoy Goswami, Kiran Bhaskaran-Nair, William A. Shelton, Bobby G. Sumpter, S. Michael Kilbey, ACS Nano 10 (7) (2016) 7008.
[30] Cheng-Kuang Lee, Chun-Wei Pao, J. Phys. Chem. C 116 (23) (2012) 12455.
[31] Cheng-Kuang Lee, Chun-Wei Pao, J. Phys. Chem. C 118 (21) (2014) 11224.
[32] Chris H. Rycroft, Chaos: Interdiscipl. J. Nonlin. Sci. 19 (4) (2009) 041111.
[33] Umar Farooq Ghumman, Akshay Iyer, Rabindra Dulal, Joydeep Munshi, Aaron Wang, TeYu Chien, Ganesh Balasubramanian, Wei Chen, J. Mech. Des. (2018).
[34] Umar Farooq Ghumman, Akshay Iyer, Rabindra Dulal, Aaron Wang, Joydeep Munshi, TeYu Chien, Ganesh Balasubramanian, Wei Chen, ASME IDETC/CIE Design Automation Conference, ASME, Quebec City, Quebec, Canada, 2018.